



Numerical Investigation of Water Addition into Intake Air in Modern Automobiles Diesel Engines

Mustafa TUTU^{1,*}, Zehra ŞAHİN², Orhan DURGUN³

¹ Karadeniz Teknik Üniversitesi, Deniz Bilimleri Fakültesi, Gemi İnşaatı ve Gemi Makineleri Mühendisliği Bölümü, Sürmene, 61530, Trabzon, Türkiye

² Karadeniz Teknik Üniversitesi, Mühendislik Fakültesi, Makine Mühendisliği Bölümü, Ortahisar, 61080, Trabzon, Türkiye

³ Avrasya Üniversitesi, Mühendislik Mimarlık Fakültesi, Makine Mühendisliği Bölümü, Yomra, 61250, Trabzon, Türkiye

ARTICLE INFO

2024, vol. 44, no.2, pp. 308-321

©2024 TIBTD Online.

doi: 10.47480/isibtcd.1563972

Research Article

Received: 02 October 2023

Accepted: 21 July 2024

* Corresponding Author

e-mail: mtuti@ktu.edu.tr

Keywords:

Thermodynamic cycle model

Water using

Heat release rate

NO emission

ORCID Numbers in author order:

0000-0002-2309-3735

0000-0002-7140-2061

0000-0001-6381-0690

ABSTRACT

In the present study, the effects of water addition into intake air (WAIA) on combustion, engine performance, and NO emission in diesel engines were investigated numerically. Here, Ferguson's thermodynamic-based zero-dimensional single-zone cycle model was used and improved with new approaches for neat diesel fuel (NDF) and WAIA. After controlling the model's accuracy for NDF and WAIA, the effects of WAIA were first investigated in the Renault K9K diesel engine. For (5 and 7.5)% water ratios (WRs), effective power decreased by 4.26% and 7.37%, brake specific fuel consumption (BSFC) increased by 6.95% and 10.56%, and NO emission reduced by 12.43% and 16.39%, respectively. In the second application, the effects of (3, 6, and 9)% WRs on combustion, engine performance, and NO emission in the Renault M9R diesel engine were investigated at 4000 rpm by using this developed model. For (3, 6, and 9)% WRs, BSFC increased by 0.97%, 3.39%, and 8.25%, and NO emission decreased by 10.31%, 17.66%, and 34.20%, respectively. For (3 and 6)% WRs effective power increased, and NO emission decreased significantly without considerable deterioration in the BSFC at 4000 rpm. Cylinder pressure values and heat release rate increased for (3 and 6)% WRs and decreased for 9% WR.

Modern Otomobil Dizel Motorlarında Emme Havaına Su Eklenmesinin Sayısal İncelenmesi

MAKALE BİLGİSİ

Anahtar Kelimeler:

Termodinamik Çevrim Modeli

Su kullanımı

Açığa çıkan ısı oranı

NO emisyonu

ÖZET

Sunulan çalışmada, dizel motorlarda emme havasına su eklenmesinin (EHSE) yanma, motor performansı ve NO emisyonu üzerindeki etkileri sayısal olarak incelenmiştir. Burada Ferguson'un termodinamik esaslı sıfır-boyutlu tek-bölgeli çevrim modeli kullanılmıştır ve söz konusu model saf dizel yakıtı (SDY) için yeni yaklaşımlarla geliştirilmiştir ve daha sonra geliştirilen çevrim modeli EHSE durumu için uyarlanmıştır. Modelin SDY ve EHSE için doğruluğu kontrol edildikten sonra, EHSE'nin etkileri ilk olarak Renault K9K dizel motorunda incelenmiştir. Seçilen %(5 ve 7.5) su oranları için; efektif güç %4.26 ve %7.37 düzeylerinde azalmış, özgül yakıt tüketimi (ÖYT) %6.95 ve %10.56 oranlarında artmış ve NO emisyonu ise %12.43 ve %16.39 düzeylerinde azalmıştır. İkinci sayısal uygulamada ise; %(3, 6 ve 9) gibi üç farklı su oranının kullanımının yanma, motor performansı ve NO emisyonu üzerindeki etkileri Renault M9R dizel motorunda 4000 d/d devir sayısında incelenmiştir. %(3, 6 ve 9) su oranları için; ÖYT, sırasıyla %0.97, %3.39 ve %8.25 oranlarında artmış ve NO emisyonu ise sırasıyla %10.31, %17.66 ve %34.20 oranlarında azalmıştır. %(3 ve 6) su oranlarında, efektif güç artmış ve NO emisyonu, ÖYT'de önemli bir kötüleşme olmadan önemli ölçüde azalmıştır. Silindirik basınçları ve açığa çıkan ısı oranları %(3 ve 6) su oranlarında artmış, %9 su oranında ise azalmıştır.

NOMENCLATURE

b_e , BSFC	brake specific fuel consumption (kg/kWh)
Ne	effective power (kW)
NDF	neat diesel fuel
Y_{NO}	mole fraction of nitrogen oxide
WAIA	water adding into the intake air

CA	crank angle
ZDSZ	zero dimensional single zone
ε	compression ratio
ID	ignition delay
HRR	heat release rate (J/deg.)

INTRODUCTION

It is well known that in modern industries possible maximum reduction of time and money spent on the development and preparation of various products and the rapid implementation of changes in product design parameters and operating modes are required. Costly and time-consuming experimental tests can be modeled under the same conditions, significantly increasing the efficiency of research and development with the improvement and implementation of various computer modeling studies (Zhang et al., 2023; Bondar et al., 2020). Modeling studies are also important and necessary for internal combustion engines, especially diesel engines which are one of the main sources of mechanical energy for propulsion of ships (seagoing ships) and land vehicles. Actually, the modeling of diesel engine cycles is an important research area from the past to the present, and various types of engine cycle models are developed and applied to calculate diesel engine cycles. In practice, by using these diesel engine cycle models and other simulation methods, the number of costly systematic experiment studies could be reduced and optimum engine design parameters can be calculated in a very short time. By this way, very useful results can be reached. Thus, these models reduce the cost and time required for engine development and help to reach the most suitable designs. Therefore, nowadays new simulation models are constantly being developed and improved (Bedford et al., 2000; Pasternak et al., 2009; Shrivastava et al., 2002; Heywood 1988; Jurić et al., 2023). In the following section, the main models applied in combustion and cycle calculations in diesel engines have been briefly introduced. Moreover; some of the results obtained from the application of these models for NDF and also for alternative fuels and for alternative solutions given in the main literature were been summarized.

Literatur Review

Various combustion types and complete cycle models have been developed for diesel engines, typically categorized as thermodynamic-based models and multi-dimensional models (MDMs) (Sahin and Durgun, 2008). Thermodynamic-based models rely on the application of the first law of thermodynamics to the engine cylinder or its manifolds, yielding a system of ordinary differential equations governing cylinder pressure, temperature, work, and heat transfer. These equations are solved to compute the diesel engine cycle accurately, facilitating the determination of engine performance parameters and exhaust emissions. Conversely, MDMs involve numerically solving fundamental differential equations governing fluid motion and combustion processes within finely meshed engine cylinders. While MDMs offer detailed spatial and temporal resolution, they demand extensive computational resources and time due to the complexity of meshing irregular combustion chamber geometries. Consequently, MDMs are primarily utilized for analyzing flow motion in non-combustible states and

optimizing combustion chamber geometry, rather than modeling entire engine cycles or determining performance parameters. Therefore, for comprehensive engine cycle calculations and parametric studies related to engine performance and exhaust emissions, thermodynamic-based models are generally preferred (Sahin and Durgun, 2008; Kökkülünk et al., 2013).

Many thermodynamic-based models (Sahin and Durgun, 2008; Kökkülünk et al., 2013; Oiang, 1992) and MDMs (Savioli, 2015; Tutak and Jamrozik, 2016) can be found in the literature. Tutak et al. (2016) improved a CFD model for a turbocharged diesel engine, confirming its accuracy with test engine data, then used it to optimize the engine cycle, noting a significant increase in NO_x and soot emissions for optimal efficiency. They emphasized its value in optimizing internal combustion engines for thermodynamic parameters and emissions.

Sahin and Durgun (2008) developed a multi-zone combustion model for NDF, ethanol, and gasoline fumigation in diesel engines, studying their effects on combustion dynamics, efficiency, and emissions. Their findings showed ethanol fumigation reduced BSFC and NO concentration, while gasoline fumigation decreased NO concentration with minimal impact on BSFC.

Many thermodynamic-based models (Sahin and Durgun, 2008; Kökkülünk et al., 2013; Oiang, 1992) and MDMs (Savioli, 2015; Tutak and Jamrozik, 2016) have been performed to calculate the diesel engine cycle for NDF, for using of alternative various fuel additives, water, etc. in the literature. These modeling studies have provided valuable information to scientists and the automotive sector. Today, numerical studies and also experimental studies for related to alternative fuel additives, improving of engine design, developing combustion process, etc. continue intensively. The main purposes of these studies are to reduce environmental pollution and to improve engine performance. Since the adding water in internal combustion engines, especially in diesel engines consists of an effective method to reduce NO_x emissions, research on this subject continues. In fact; since the 1950s, adding water in different ways in diesel engines has been attracted the interest of many scientists and a lot of numerical and experimental studies have been carried out on this subject. In recent years, the number of numerical studies on using of alternative fuels and water in diesel engines has increased, especially with the increase in the speed and capacity of computers (Sahin and Durgun, 2008; Kökkülünk, 2012; Lamas et al., 2013; Gonca et al., 2015; Sandeep et al., 2019; Tamma et al., 2003). Some examples of numerical studies on the adding of water or various water-alternative fuels in diesel engines can be summarized as follows:

Bedford et al. (2000) explored cylinder water injection's impact on diesel engine performance using Kiva-3v based CFD simulations, finding that it lowered NO_x emissions and soot formation due to water evaporation and increased gas specific

heat around the flame. Sandeep et al. (2019) investigated the impact of water addition into intake air (WAIA) on engine performance and emissions in a turbocharged diesel engine, employing both experimental and numerical methods. Simulations were carried out using a one-dimensional package computer program (DPCP) for different water injection amounts, revealing that increased injection reduced NO_x emissions but increased smoke levels. Optimal performance was observed with 2.8 mg of water injection, leading to a notable decrease in cylinder temperature and an 8-10% reduction in NO_x emissions, despite a 20% increase in smoke. Kannan and Udayakumar (2009) developed a thermodynamic-based ZDSZ model to investigate the effects of water emulsion on cylinder pressure, engine performance, and NO concentration. Their study reveals that water emulsion increases BSFC but decreases NO concentration. Kökkülünk et al. (2013) investigated the effects of water addition into the intake air as steam on engine performance and exhaust emissions through experimental and numerical methods. In their numerical analysis, Ferguson's (1986) thermodynamic-based ZDSZ cycle model was refined and adapted for a 20% water-steam ratio. Employing an electronically controlled injection system, water was introduced into the intake air as steam. Their findings revealed that steam injection improved engine performance and reduced NO emissions, with no significant impact on CO, CO₂, and HC emissions. As can be seen from the above literature survey, many studies have been carried out, including dimensional package computer programs and thermodynamic-based ZDSZ models to calculate diesel engine cycles for NDF, various alternative fuels, and different water adding applications. Although there are many studies on the modeling of NDF (Pasternak et al., 2009; Shrivastava et al., 2002; Sindhu et al., 2014) and different alternative fuels (Nemati et al., 2016; Rakopoulos et al., 2008) studies on the numerical examination of water adding in diesel engines are more limited. In fact, the experimental investigation of water adding in diesel engines has been carried out widely. In these studies; researchers generally have preferred three different methods for the application of water in diesel engines. These methods can be classified as adding of water into the intake air, mixing of the water with the diesel fuel, as known as the emulsion method, and injection of the water directly into the combustion chamber with a separate injector. Water adding in diesel engines by these three methods has been explained to be very effective in reducing NO_x emissions (Gowrishankar et al., 2020; Jhalani et al., 2023; Ece and Ayhan, 2019). Zhu et al. (2019) made the following statements about the water adding in internal combustion engines in their review research. Water adding is a promising technique to reduce the cylinder temperature and exhaust temperature, mitigate combustion knock, improve combustion phasing and decrease NO_x emissions. Also, they stated that since mechanisms of water injection with different aims are distinct, benefits on engine performances and emissions are also varied.

Out of these; considering the NO_x emission reduction potential of water adding, nowadays water has been preferred to use with the above-explained methods as a third additive along with the other alternative fuels in diesel engines (Wang et al., 2018; Vellaiyan et al., 2019; Maawa et al., 2020). For example, Maawa et al. (2020) experimentally investigated the effects of biodiesel-diesel fuel blends (B20) emulsified with varying proportions of water on engine performance, combustion characteristics, and exhaust emissions. They utilized conventional diesel fuel, blended

palm oil methyl ester/diesel fuel (B20), and B20 emulsified with different water proportions (B20E5, B20E10, B20E20, and B20E30) in their study. Their findings suggest that water emulsification with biodiesel-diesel fuel blends effectively reduces exhaust emissions, particularly NO_x, without compromising engine performance.

Our literature review confirms that water adding is one of the best methods that can be applied to reduce NO_x emissions in diesel engines. Therefore, it is worthwhile important to numerically and experimentally examine the effects of water adding on combustion, engine performance parameters, and exhaust emissions in current automotive diesel engines. Besides, as can be stated from the above brief literature review modeling studies on water adding are more limited than experimental studies. For this reason, in the present study, the water adding into the intake air has been numerically investigated in two different diesel engines, used by current automobiles. Also, an experimental investigation of WAIA in an automotive diesel engine has been carried out and the experimental data have been compared with numerical results. Here, to calculate the diesel engine cycle, thermodynamic-based ZDSZ model, which is practical and easy to implement, was improved and applied for NDF and WAIA. In this model, modeling of the intake and exhaust processes, which are not usually calculated in the cycle calculations in the literature, were also performed. Then, the mentioned model was adapted for water adding to the intake air with new suppositions, and the accuracy control of this program was verified by comparing with the experimental data and by numerical results of the studies given in the literature. Also, systematic numerical applications were carried out to understand the effects of WAIA on the combustion process, engine performance, and NO concentration for two different automobile diesel engines, using in road vehicles today. Thus, the results obtained from this study can be transferred directly to the automotive industry. More importantly, the present study fills a critical research gap by developing and using a thermodynamic-based ZDSZ model to investigate the effects of WAIA on engine performance and NO emissions in automotive diesel engines.

BRIEF DESCRIPTION OF PRESENT MODEL FOR NDF

In the present study, a thermodynamic-based single-zone model for calculating the complete diesel engine cycle is adapted and improved. Here, intake and exhaust processes are modeled with a practical calculation method developed by Durgun (1991). Compression, combustion, and expansion processes were computed by adapting the model originally developed and given by Ferguson (1986). Firstly, the above-mentioned complete diesel engine cycle model was improved for NDF, and its accuracy was checked. Then, this model has been adapted for the WAIA.

a) Modeling of Intake and Exhaust Processes: Intake and exhaust processes are modeled with a practical calculation method developed by Durgun (1991). This model will be introduced very briefly here. Detailed information on this subject can be found in the reference (Durgun, 1991). The pressure at the intake process was calculated using the following relation by applying the well-known Bernoulli equation to the engine intake system.

$$P_a \text{ (MPa)} = P_c' - (\beta^2 + \xi) \left[\frac{V_{m,n}}{n_N} \right]^2 \cdot \frac{P_a}{2} \cdot 10^{-6} \quad (1)$$

where P'_c is turbocharger compressor outlet pressure, $(\beta^2 + \xi)$ is the coefficient showing the total losses in the intake system, n and n_N are the actual engine speed and nominal engine speed, respectively, V_m is the maximum flow speed in the intake system, ρ_a is the density of air. Here, since turbocharged diesel engines are used, the

pressure and temperature at the outlet of the compressor of the turbocharger were determined by using the semi-empirical relation (2) and (3) given in Table 1. Also, residual gases have been taken into account by using γ_r the coefficient of the residual gases in the present model and γ_r was calculated by using relation (4) given in Table 1.

Table 1. Some relations used in the intake and exhaust process calculation

Equation	and	equation number	Explanation of some parameters in the relations
P'_c (MPa) = 1.5 P_0	low-turbocharged	(2a)	P_0 : Ambient pressure
P'_c (MPa) = (1.5-2.2) P_0	mid-turbocharged	(2b)	
P'_c (MPa) = (2.2-2.5) P_0	high-turbocharged	(2c)	
T'_c (K) = $T_0 \cdot \left(\frac{P'_c}{P_0}\right)^{\frac{n_c-1}{n_c}}$		(3)	T_0 : Ambient temperature n_c : Polytropic compression exponent of the compressor
$\gamma_r = \frac{T'_c + \Delta T}{T_r} \cdot \frac{\varphi_s \cdot P_r}{\varepsilon \cdot \varphi_{ed} \cdot P_a - \varphi_s \cdot P_r}$		(4)	φ_{ed} : Additional charge coefficient φ_s : Scavenging coefficient of supercharged ε : Compression ratio of the engine ΔT : Amount of preheating of the intake charge T_r : Temperature of the exhaust gases
$\left. \begin{array}{l} P'_c = P_0 \\ T'_c = T_0 \end{array} \right\}$	for naturally aspirated engines		
$T'_r = \frac{T_b}{\sqrt[3]{P_b/P_r}}$, $\left \frac{T'_r - T_r}{T_r} \right \leq 3\%$		(5a, 5b)	T'_r : The calculated exhaust temperature P_r, T_r : The selected exhaust gas pressure and temperature T_b, P_b : Temperature and pressure at the end of the expansion stroke
$T_r = (600 - 1000)K$			
$P_r = (0.75 - 0.98)P'_c$			

The temperature at the end of the exhaust process was calculated by using relation (5a) given in Table 1, depending on the temperature at the end of the intake. The exhaust gas temperature calculated at the end of the cycle calculations is compared with the selected exhaust gas temperature at the beginning of the cycle. If the difference between the two values is less than 3%, the cycle calculations and empirical data selections can be considered compatible. This difference ratio can be called as the accuracy of the cycle. If the difference exceeds this value, the cycle might be repeated by taking the last calculated exhaust gas temperature as the residual gas temperature value. The cycle calculation continues iteratively until the difference becomes less than %3. Thus, complete cycle calculation control has been reached. Exhaust temperature comparison procedure is carried out by using relation (5b) given in Table 1.

b) Modeling of Compression, Combustion and Expansion Processes:

Applying the first law of thermodynamics to the gas mixture in the cylinder, the following set of differential equations can be obtained by applying the energy balance where work, heat losses, and mass losses are also considered. This set of differential equations in question is solved from the beginning of the compression process to the end of the expansion process step by step and the cylinder pressure, cylinder temperature, and cycle work values are determined. Here, the set of ordinary differential equations numbered (6-11) is solved simultaneously by Butcher's (1995) 5th Order Runge-Kutta method during the compression, combustion and expansion processes. Detailed information on the deriving of these equations can be found in the references (Tuti, 2022; Ferguson, 1986). Also, at the end of a step, cylinder temperature and pressure values were calculated the next crankshaft angle by using (12) and (14) equations, given in Table 2. These equations were solved by Newton-Raphson method in 0.5° CA steps.

$$\frac{dm_a}{d\theta} = -\frac{1}{\omega} \cdot \left(\frac{\dot{m}_1}{1 + \phi \cdot F_s} \right) \quad (6)$$

$$\frac{dm_f}{d\theta} = \frac{1}{\omega} \cdot \left(\dot{m}_{f,i} - \frac{\dot{m}_1 \cdot \phi \cdot F_s}{1 + \phi \cdot F_s} \right) \quad (7)$$

$$\frac{dU}{d\theta} = -\frac{\dot{Q}_l}{\omega} - P \cdot \frac{dV}{d\theta} + \frac{\dot{m}_f \cdot h_f}{\omega} - \frac{\dot{m}_1 \cdot h_1}{\omega} \quad (8)$$

$$\frac{dW}{d\theta} = P \cdot \frac{dV}{d\theta} \quad (9)$$

$$\frac{\dot{Q}_l}{\omega} = \frac{h \left(\frac{\pi B^2}{2} + \frac{4V}{B} \right) (T - T_w)}{\omega} \quad (10)$$

$$\frac{\dot{m}_1 \cdot h_1}{\omega} = \frac{C \cdot m \cdot h_1}{\omega} \quad (11)$$

Eq.6 and Eq.7 give the rates of change of the masses of air and fuel in the cylinder in respect of the crankshaft angle. In these equations, \dot{m}_1 is the loss of mass escaping from the valves and piston rings, $\dot{m}_{f,i}$ is the total mass of fuel to be injected, ϕ is the equivalence ratio, and F_s is the stoichiometric fuel-air ratio. Eq.8 is the first law of thermodynamics or the energy equation for a closed system which is applied to the cylinder contents during compression, combustion, and expansion strokes. The terms on the right-hand side of this equation show heat transfer, work, energy provided by injected fuel, and blowby, respectively. The work, heat transfer, and blowby have been modeled by using relations (9-11), respectively.

In Eq.10, B is the cylinder bore, T_w is the wall temperature, V is the volume of cylinder and h is the convection heat transfer coefficient of the gas in the cylinder. Here, h has been determined from Woschni's (1967) correlation.

In Eq.11, \dot{m}_1 is the mass flow rate of gas escaping from the rings and valves, C is the blowby coefficient. Thus, as explained above $V, \dot{m}_a, \dot{m}_f, U, W, \dot{Q}_l$ and h_1 values can be determined numerically by solving this ordinary differential equation system. Here U internal energy, V the cylinder volume, and h enthalpy values in the differential equations have been calculated in the following forms by using Olikara and Borman (1998) method.

Table 2. The used equations for calculation of cylinder temperature and pressure.

$T_{i+0.5} = T_i + \Delta T$	(12)
$\Delta T = \frac{-V \left[\frac{10 \left(\frac{du}{d\theta} \right) + \frac{dv}{d\theta} \left(\frac{\partial \ln v}{\partial \ln T} + \frac{\partial \ln v}{\partial \ln P} \right) \right]}{\frac{V^2}{T} \left[\left(-\frac{10c_p T}{pV} + \frac{\partial \ln v}{\partial \ln T} \right) \left(-\frac{\partial \ln v}{\partial \ln P} \right) + \frac{\partial \ln v}{\partial \ln T} \left(\frac{\partial \ln v}{\partial \ln T} + \frac{\partial \ln v}{\partial \ln P} \right) \right]}$	(13)
$P_{i+0.5} = P_i + \Delta P$	(14)
$\Delta P = \frac{\frac{pV}{T} \left[\frac{10c_p T}{pV} \frac{\partial \ln v}{\partial \ln T} \frac{dv}{d\theta} - \frac{10 \left(\frac{du}{d\theta} \frac{\partial \ln v}{\partial \ln T} \right)}{p} \right]}{\frac{V^2}{T} \left[\left(-\frac{10c_p T}{pV} + \frac{\partial \ln v}{\partial \ln T} \right) \left(-\frac{\partial \ln v}{\partial \ln P} \right) + \frac{\partial \ln v}{\partial \ln T} \left(\frac{\partial \ln v}{\partial \ln T} + \frac{\partial \ln v}{\partial \ln P} \right) \right]}$	(15)

After determining the complete diesel engine cycle, engine performance parameters such as effective power, effective efficiency, and BSFC are calculated from the relationships given by Heywood (1988) and Durgun (1991, 2022). For example; in the present study, effective engine characteristics have been computed by using the following semi-empirical mean effective pressure relationship given by Durgun (1991, 2022), while here and in the literature generally indicated engine characteristics have been obtained.

$$P_{m,m}(\text{MPa}) = 10 \cdot (a + b \cdot V_{p,m}) \frac{P'_c}{P_{m,i}} \quad (16a)$$

$$P_{m,e}(\text{MPa}) = P_{m,i} - P_{m,m} \quad (16b)$$

In Eq. 16a and Eq.16b, $P_{m,i}$ is the mean indicated pressure, and $V_{p,m}$ is the mean piston velocity. a and b are coefficients depending on the engine type and for the Renault K9K 700 type test engine and Renault Talisman M9R type engine, these values of a and b were selected as 0.089 and 0.0118, $P_{m,i}$ value has been calculated as follows by using cycle data ($P_{m,i}=W/V$).

The Adaptations of the Present Model for WAIA

a) The temperature at the end of the intake process: In the present study, the developed cycle model for NDF is adapted to WAIA by applying some modifications. In the WAIA experiment, water can be introduced into the air charge by using a simple carburetor. Thus, the temperature at the end of the intake process decreases

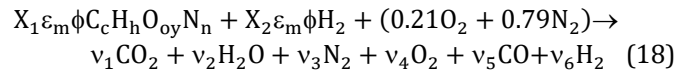
because of water vaporization in the intake manifold. The decrease in the temperature has been calculated by using of the following relation.

$$T_{a,WAIA}(\text{K}) = \frac{T'_c + \Delta T + \gamma_r \cdot T_r}{T_r} - \frac{M_w \cdot Q_w}{M_1 \cdot c_p} \quad (17)$$

Here, Q_w is the heat of evaporation or latent heat of the water, M_w is the mole number of the water added into the inlet channel for 1 kg diesel fuel, and M_1 is the mole number of the fresh charge.

b) Calculation of the thermodynamic properties of the mixture at low temperature:

For WAIA, water, air, and residual exhaust gases are compressed during the compression process. Therefore, the following combustion reaction was used to determine the thermodynamic properties of the mixture, such as enthalpy, and specific heat, in the cylinder at low temperatures. For this, first of all, the mole fractions of combustion products formed at low temperatures were determined. In Table 3, the number of moles and mole fraction of the combustion products formed at low temperatures are given (Ferguson 1986).



where $X_1 \varepsilon_m \phi$ and $X_2 \varepsilon_m \phi$ are the amount of diesel fuel added per 1 mol air, and the amount of water added per 1 mol of air respectively. Also, here X_1 and X_2 are the volumetric percentages of diesel fuel and water in the mixture, respectively. The term of ε_m is the amount of oxygen required to burn 1 mol of fuel and it has been calculated by using the following simple relation $\varepsilon_m = (c+h/4-oy/2)$. Here c , h , and oy are the atomic numbers of carbon, hydrogen, and oxygen in the chemical formula of the fuel.

After determining the mol fractions of each substance in the mixture by this way, the thermodynamic properties of the mixture were calculated using Ferguson (1986) ve Heywood (1988) references.

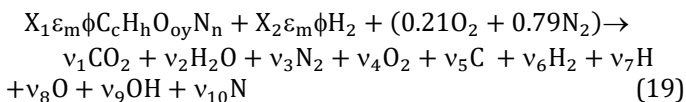
Table 3. v_i mol numbers and y_i mol fraction ratios for WAIA at low temperature (Tuti, 2022).

Products	v_i (mol/mol air)	$\phi < 1$	mole fractions, $y_i = v_i/n_t^*$
CO ₂	v_1	$X_1 \cdot \varepsilon_m \cdot \phi \cdot c$	$y_{CO_2} = (X_1 \cdot \varepsilon_m \cdot \phi \cdot c)/n_t$
H ₂ O	v_2	$X_1 \cdot \varepsilon_m \cdot \phi \cdot h/2 + X_2 \cdot \varepsilon_m \cdot \phi$	$y_{H_2O} = (\varepsilon_m \cdot \phi \cdot (X_1 \cdot h/2 + X_2))/n_t$
N ₂	v_3	$X_1 \cdot \varepsilon_m \cdot \phi \cdot n/2 + 0.79$	$y_{N_2} = (X_1 \cdot \varepsilon_m \cdot \phi \cdot n/2 + 0.79)/n_t$
O ₂	v_4	$0.21(1 - \phi X_1)$	$y_{O_2} = 0.21(1 - \phi X_1)/n_t$
CO	v_5	0	
H ₂	v_6	0	

* n_t is the total mol number of combustion products formed at low temperatures.

c) Calculation of the thermodynamic properties of the mixture at high temperature:

For the WAIA, the combustion equation is arranged as follows to calculate the mol numbers of the combustion products during the combustion process (Ferguson, 1986).



where $v_1, v_2, v_3, v_4, v_5, v_6, v_7, v_8, v_9$, and v_{10} are the mole number of the combustion products and they have been determined by using Olikara's (1998) method. Once the combustion products are determined, the thermodynamic properties and their derivatives with respect to temperature, pressure, and equivalence ratio can be calculated. Detailed information on this subject can be found in the references such as Tuti (2022) and Ferguson (1986).

RESULTS AND DISCUSSION

The Accuracy Control of the Developed Model for NDF and WAIA

Here, firstly, the numerical results obtained from the present model for NDF are compared with the experimental and thermodynamic model results of Rajak et al. (2018). Rajak et al. (2018) used in their numerical studies, a professional ready-made package computer program prepared as a thermodynamic-based multi-zone combustion model. In Fig. 3(a) and (b), cylinder pressure and HRR values obtained from the present model are compared with the experimental and thermodynamic model results of Rajak et al. (2018) for 18.5 compression ratio under full load at 1500 rpm. It can be seen from Fig. 3(a) that, the tendencies of Rajak et al.'s (2018) numerical and experimental pressure curves are similar to that of the present model. The maximum cylinder pressure values of the experiments and model of Rajak et al. (2018) are given 87.15 bar at 11.37 °CA, and 90.13 bar at 2.42 °CA, respectively. However, the maximum cylinder pressure value has been calculated as 86.80 bar at 8 °CA by using the present model. Thus, the difference of the present model in respect to Rajak's (2018) model and experimental results for maximum cylinder pressure was 3.42%. On the other hand, the difference between the maximum pressure value obtained from the present model and Rajak's (2018) experiment has been determined as 0.402%. Hence, it can be said that the maximum pressure value obtained from the developed model is closer to Rajak's (2018) experimental result than that of Rajak's (2018) model.

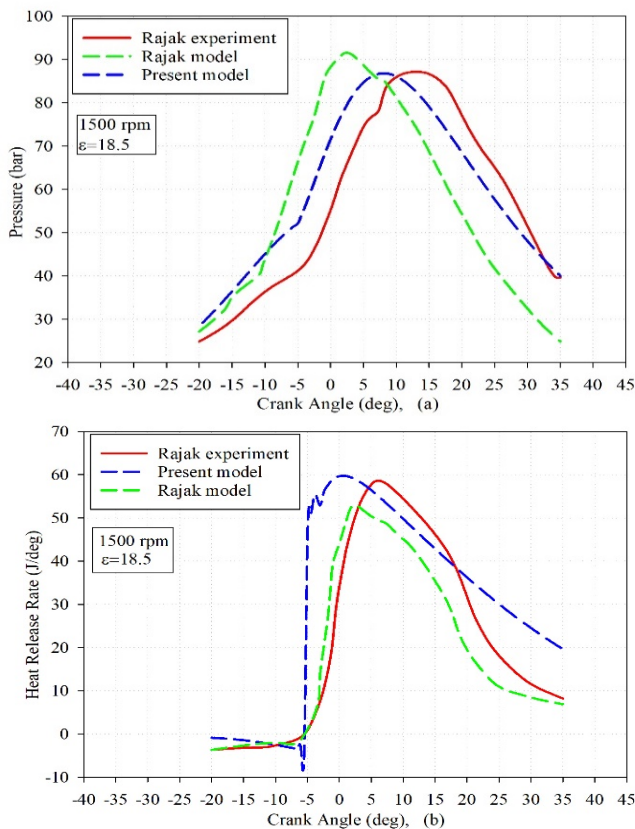


Fig. 3. Comparison **a)** cylinder pressure and **b)** HRR values obtained from the present model with the experimental and model results of Rajak et al. (2018).

HRR curves with respect to various crank angles for the present model and Rajak's (2018) experimental and theoretical results are shown in Fig. 3(b). As can be seen in this figure, the tendency of the HRR curve obtained in this model

and the tendency of Rajak's (2018) experimental and numerical HRR curves are most similar. The maximum value of HRR calculated from the present model and the experimental and model results from Rajak et al. (2018) are 59.77 J/deg at 0.5 °CA, 58.34 J/deg at 5.43 °CA and 53.06 J/deg at 2.29 °CA, respectively. The difference between Rajak's (2018) model and experimental maximum HRR values was found as 8.12%. However, the maximum HRR value obtained from our model is closer to Rajak's (2018) experimental HRR and the difference was found to be 2.44%. Thus, it is clear from Fig. 3(a) and (b) that our model results are in good agreement with Rajak's (2018) experimental results than that of their own results. The values and comparison results of effective efficiency obtained from the developed model and Rajak et al.'s (2018) model and experimental results are shown in Table 4. As can be seen from this table, effective efficiency in the present model was determined as 31.63%. Rajak et al.'s (2018) experimental and numerical effective efficiency values were given as 32.5%, and 32.59%, respectively. Here, there is a 0.277% difference between Rajak et al.'s (2018) model and their experimental effective efficiency values. However, there is a 2.667% difference between our model result and the experimental value of Rajak et al. (2018). Possible reasons for this difference can be explained as follows. In the present model, it is assumed that all of the fuel is injected into the cylinder as the main injection. That is to say, pilot and main fuel injections are not taken into account separately in the present model.

In addition, it is also assumed that the injected fuel burns immediately and detailed calculations of the penetration, evaporation, and disintegration of the sprayed fuel have not been taken into account. In fact, the 2.667% difference can be considered an acceptable error level, and it can be said that the predicted results by our model agree reasonably with the Rajak et al. (2018) data.

In another numerical application, the results of the present model were compared with experimental results performed by authors for NDF, 6%, and 10% water adding ratios (WRs) at 2000 rpm and 4000 rpm under full throttle. The experimental and numerical variations of cylinder pressure, cylinder temperature, and HRR are comparatively presented in Fig. (4-7). Also, experimental and numerical values of engine torque, effective power, BSFC, and effective efficiency are given in Tables (5-6). It can be seen from these figures, the tendencies of the pressure, temperature, and HRR curves obtained from this model for NDF, 6%, and 10% WRs at 2000 and 4000 rpms are quite similar to that of experimental. The maximum pressure determined by applying the developed model for the test engine is 155.288 bar and it occurred at 8 °CA and the maximum pressure measured is 155.288 bar at 8 °CA for 6 % WR at 2000 rpm. Thus, it can be seen that the difference between maximum pressure is 1.11%. Similarly, the maximum numerical and experimental temperature values for the same conditions are 2053 K at 22.18 °CA and 2015 K at 19.5 °CA, respectively, and thus the difference ratio between maximum temperatures has been 1.85%. HRR values are also reasonably close to each other and the difference between experimental and model data for maximum HRR values has been calculated as 4.25%. However, as can be seen in Fig. 4(c), combustion started earlier in the model and the HRR curve is slightly shifted to the left than that of the test results. Possible reasons of this situation can be explained as follows.

Table 4. Comparison of the HRR, effective efficiency, and peak cylinder pressure obtained from the present model with the experimental and numerical results of Rajak et al. (2018).

$\varepsilon=18.5$	Rajak's exp.	Rajak's model	Present model	Diff. Rajak' exp. and model (%)	Diff. Rajak' exp. and present model (%)
HRR, J/deg	58.34	53.06	59.77	9.050	-2.451
η_e , %	32.5	32.59	31.63	-0.277	2.677
P_{max} , bar	87.15	90.13	86.8	-3.419	0.402
$dP/d\theta_{max}$	5.45	5.3	4.63	2.752	15.045

As explained above, in the developed model, it is assumed that all of the fuel is injected in the main combustion phase and the injected fuel burns immediately. In addition, phenomena such as the penetration of the injected fuel in the combustion chamber, the evaporation of the droplets, etc. could not be taken into account. As a result, the variations of the experiment and numerical HRR curves have been somewhat different. Similarly, acceptable proximity for cylinder pressure, temperature, HRR, and engine performance parameters values occurred for 10% WR at 2000 rpm as can be seen in Table 5. As can be shown in this table, the results of engine performance parameters calculated from the developed numerical model for 6% and 10% WRs at 2000 rpm are also very close to the

experimental data. The results of cylinder pressure, temperature, and HRR at 4000 rpm for NDF, 6%, and 10% WRs under full load conditions are shown in Fig. (6) and Fig. (7) and engine performance parameters results for the same conditions are also given in Table 6.

As can be seen from these figures and table, the model results are found to be in good agreement with the experimental results. Therefore, it can be concluded that the present model can reasonably predict the complete cycles of diesel engines for NDF and WAIA. Also, as can be seen in the Fig. (4-7)(b), WAIA decreases the cylinder temperatures for 6% and 10% WRs at 2000 and 4000 rpms

Table 5. Comparison of engine performance parameters, cylinder, temperature, and HRR calculated from the developed model for 6% and 10% WRs at 2000 rpm with the experimental results of Sahin, Durgun, and Tuti (2018, 2012).

2000 rpm	NDF			6% WR			10% WR		
	Exp.	Model	Diff. %	Exp.	Model	Diff. %	Exp.	Model	Diff. %
M_d (Nm)	144.068	152.635	-5.94	149.935	151.00	-0.71	150.413	148	1.60
N_e (kW)	30.173	31.968	-5.95	31.823	31.502	1.01	31.486	31.067	1.33
b_e (kg/kWh)	0.215	0.223	-3.72	0.221	0.210	4.99	0.226	0.216	4.31
η_e (%)	39.9	38.5	3.51	38.4	40.2	-4.71	37.51	39.05	-4.11
P_{max} (bar)	155.832	156.011	0.11	157.025	155.288	1.11	156.516	154.634	1.20
HRR_{max} (J/deg.)	55.272	52.077	5.78	54.389	51.177	4.25	54.195	50.395	7.01
T_{max} (K)	2168	2062	4.93	2053	2015	1.85	2028	1998	1.48

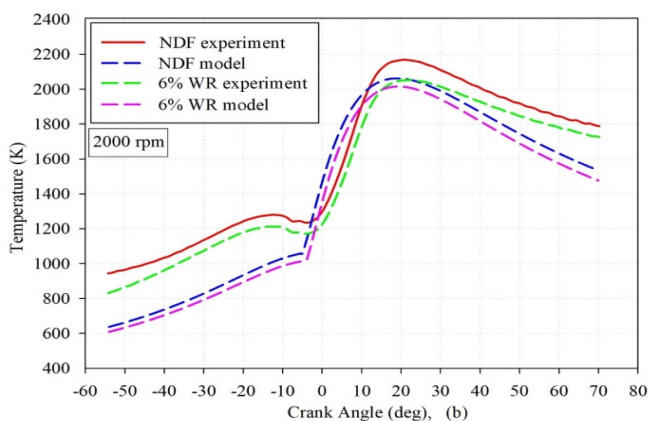
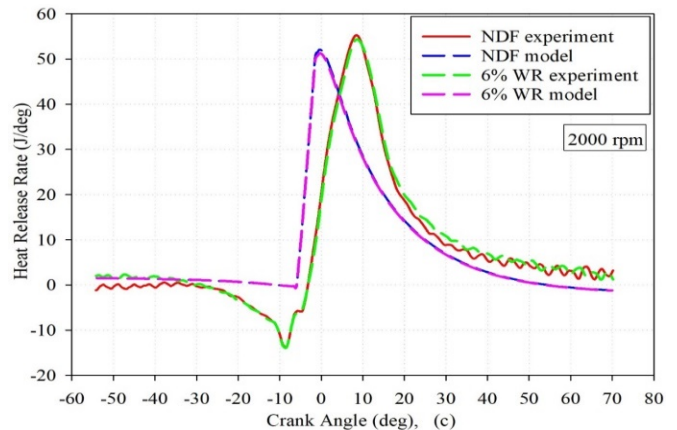
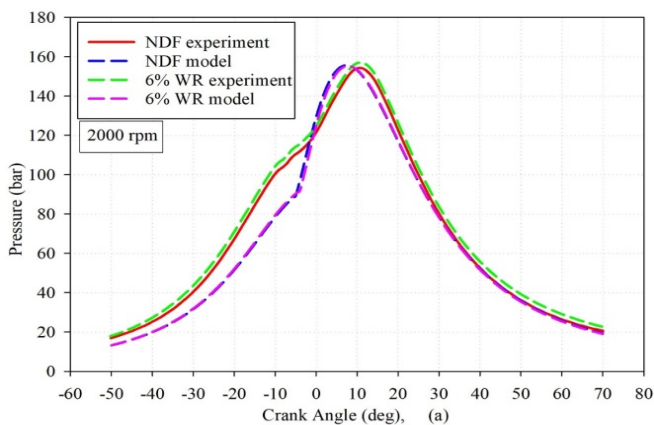


Fig. 4. Comparison a) cylinder pressure, b) cylinder temperature, and c) HRR variations of the present model for 6% WR at 2000 rpm with the experimental results of Sahin, Durgun, and Tuti (2018) and Tuti (2012).

Similar results were found in the relevant studies in the literature (Sindhu et al., 2014; Tauzia et al., 2010; Ma et al., 2014). Tauzia et al. (2010) stated that the evaporation of water in the combustion chamber and dilution of the existing mixture with the additional water causes a decrease in the temperatures of the cylinder gas content. As a result of this, it can be guessed that lower cylinder temperatures may reduce NO_x emissions (Heywood, 1988; Khatri and Goyal, 2020; Subramanian, 2011). Thus, from the following numerical applications, it can be said that WAIA reduces NO_x .

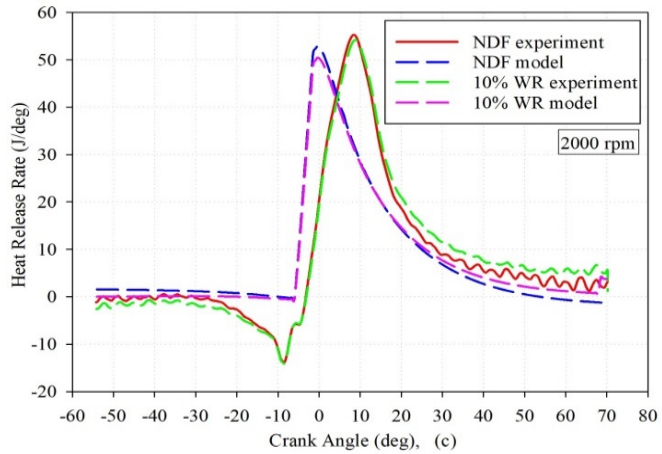
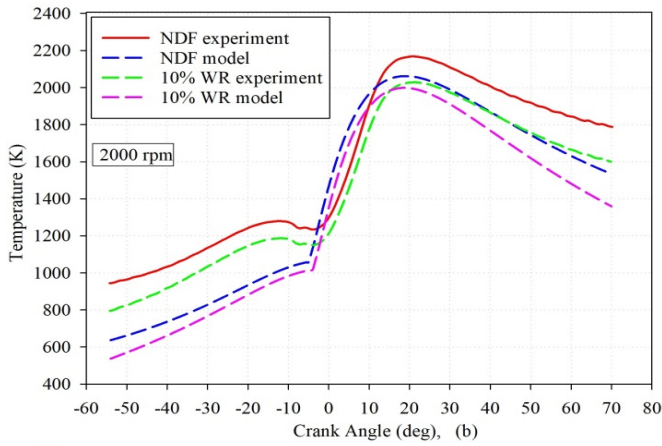
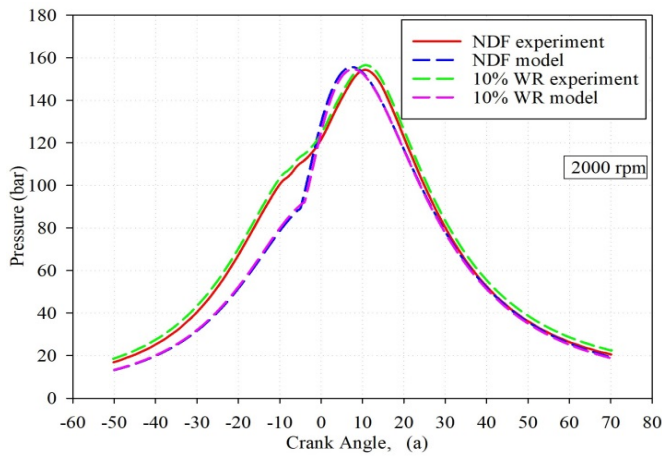


Fig. 5. Comparison **a)** cylinder pressure, **b)** cylinder temperature and **c)** HRR variations of the present model for 10% WR at 2000 rpm with the experimental results of Sahin, Durgun, and Tuti (2018) and Tuti (2012).

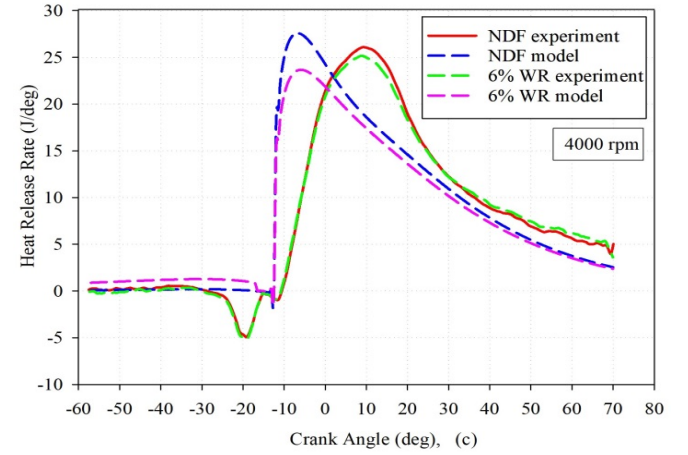
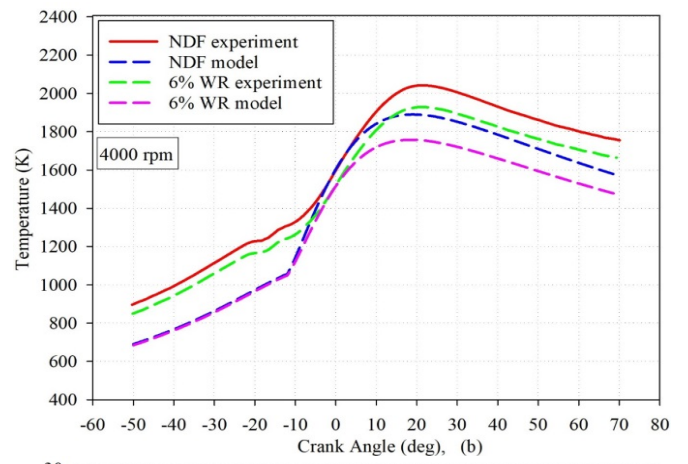
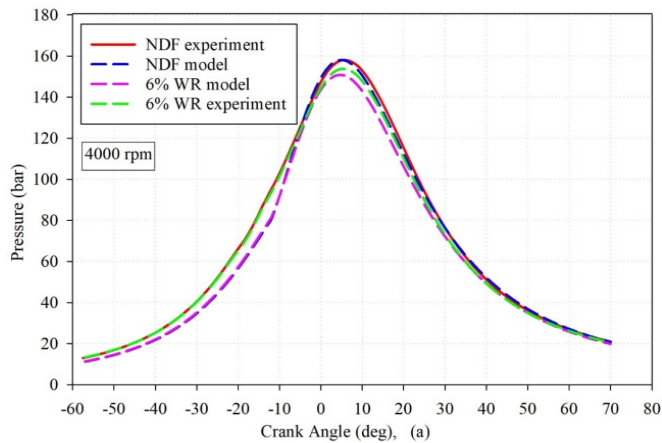
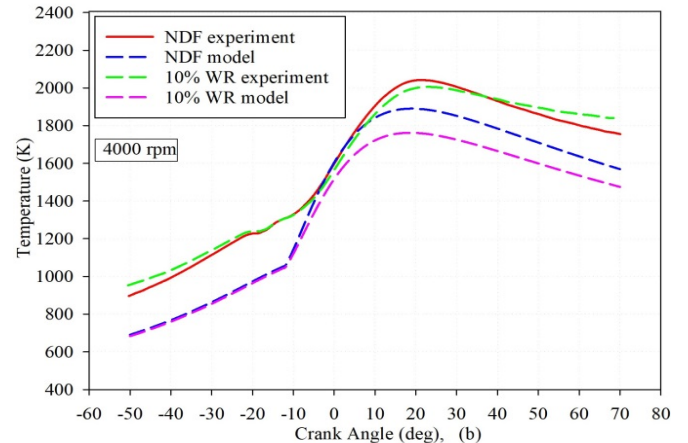
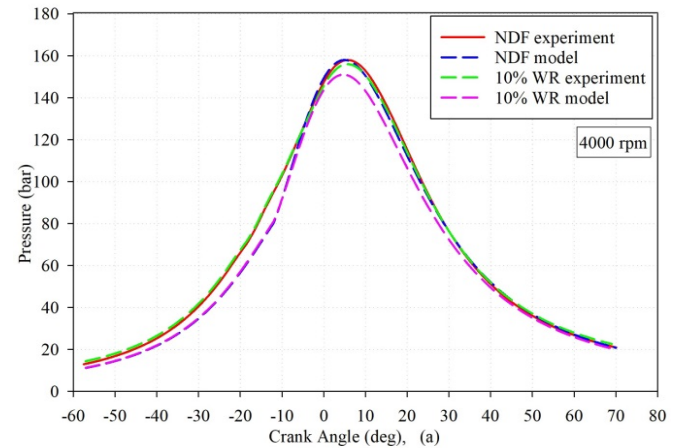


Fig. 6. Comparison **a)** cylinder pressure, **b)** cylinder temperature and **c)** HRR variations of the present model for 6% WR at 4000 rpm with the experimental results of Sahin, Durgun, and Tuti (2018) and Tuti (2012).



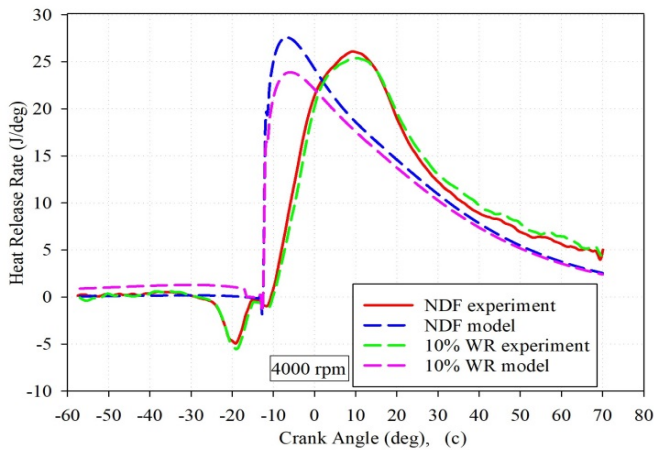


Fig. 7. Comparison **a)** cylinder pressure, **b)** cylinder temperature and **c)** HRR variations of the present model for 10% WR at 4000 rpm with the experimental results of Sahin, Durgun, and Tuti (2018) and Tuti (2012).

Table 6. Comparison of engine performance parameters, cylinder pressure, temperature, and HRR calculated from the developed model for 6% and 10% WRs at 4000 rpm with the experimental results of Sahin, Durgun, and Tuti (2018) and Tuti (2012).

4000 rpm	NDF			6% WR			10% WR		
	Exp.	Model	Diff. %	Exp.	Model	Diff. %	Exp.	Model	Diff. %
M_d (Nm)	117.980	119.280	-1.10	116.016	114.542	1.27	114.108	112.789	1.15
N_e (kW)	49.394	49.964	-1.15	48.596	47.979	1.25	47.732	47.245	1.02
b_e (kg/kWh)	0.264	0.269	-1.17	0.274	0.265	3.28	0.260	0.273	-5.04
η_e (%)	32.0	31.4	1.87	31.2	32.2	-3.21	32.7	30.9	5.31
P_{max} (bar)	157.994	158.032	0.02	154.741	151.808	1.89	156.053	151.018	3.23
HRR _{max} (J/deg.)	26.079	27.572	-5.72	25.160	23.667	5.78	25.407	23.884	5.99
T_{max} (K)	2041	1898	7	1928	1758	8.82	2005.64	1762.10	12.14

Renault K9K-700 Type Diesel Engine

As can be seen from Fig. 8(a), the maximum pressure values for NDF, 5%, and 7.5% WRs were determined as 156.243, 154.267, and 153.145 bar, respectively. By inspection of this figure, it can be said that WAIA decreases cylinder pressure. For 5% and 7.5% WRs, the reduction ratios in maximum pressure values compared to NDF have been obtained as 1.26% and 1.98%, respectively. Similar results are also reported in the relevant literature. For example, Ma et al. (2014) determined that WAIA reduces cylinder pressure and temperature. Also, WAIA decreases cylinder temperature values, as can be seen in Fig. 8(b). For example, the maximum temperature values for NDF, 5% and 7.5% WR were determined as 1973.98 K, 1917.25 K, and 1896.74 K, respectively. Thus, reduction ratios of the maximum temperatures for 5% and 7.5% WRs compared to NDF were computed as 2.87% and 3.91%, respectively. The variations of HRR for NDF, 5%, and 7.5% WRs have also been shown in Fig. 8(c) the maximum values of HRR for NDF, 5%, and 7.5% WR have been determined as 42.11 J/deg, 40.23 J/deg, and 39.49 J/deg, respectively. From this figure, it can be said that WAIA reduces HRRs. For 5% and 7.5% WRs, the maximum HRR values are reduced by 4.46% and 6.22%, respectively, compared to NDF. The probable reason of this result might be arisen from heat losses, which occurred by evaporation of latent heat of the water.

Table 7 shows the effects of WAIA on the effective power, BSFC, ignition delay (ID), and volumetric ratio of NO emission. Here, NO emission has been calculated by applying the chemical equilibrium mechanism, given by Olika and Borman (1998) using maximum combustion

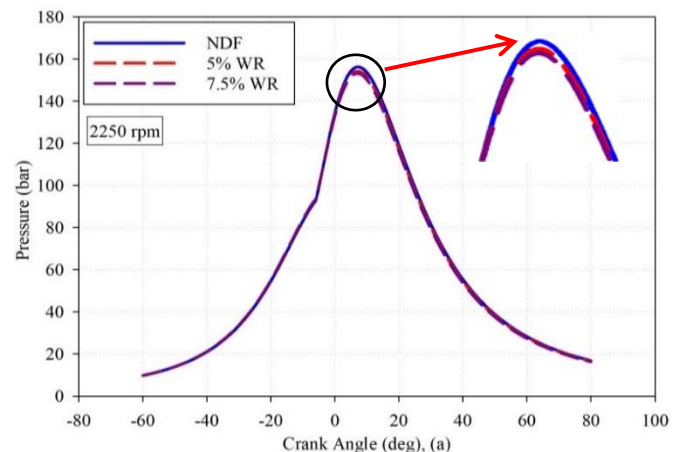
Numerical Evaluation of the Use of WAIA in Current Automotive Diesel Engines

In this paragraph, firstly, the developed computer code has been run for NDF, 5%, and 7.5% WRs at 2250 rpm, which could not be tested for the Renault K9K-700 type diesel engine, and the obtained experimental results are presented below in tables and graphics. By this way, the effects of WAIA on the Renault M9R type diesel engine, used in the Talisman model automobile were investigated numerically, and reached results have been presented and evaluated.

temperature. In Table 7, the improvements and worsening effects of WAIA on the engine performance and NO are shown in green and yellow colors respectively. For NDF, 5%, and 7.5% WRs, the effective power values were determined as 36.793 kW, 35.227 kW, and 34.081 kW, respectively. Thus, effective power values for 5% and 7.5% WRs have decreased by 4.26% and 7.37%, respectively, compared to NDF.

Table 7. Effective power, BSFC, NO and ID values for NDF, 5% and 7.5% WRs at 2250 rpm

2250 rpm, WRs	N_e (kW)	b_e (g/kWh)	γ_{NO}^{*1000}	T_{max} (K)	ID (°CA)
NDF	36.793	216.33	5.191	1973.98	2.096115
5% WR	35.227	231.38	4.546	1917.25	2.098760
7.5% WR	34.081	239.17	4.340	1896.74	2.098664



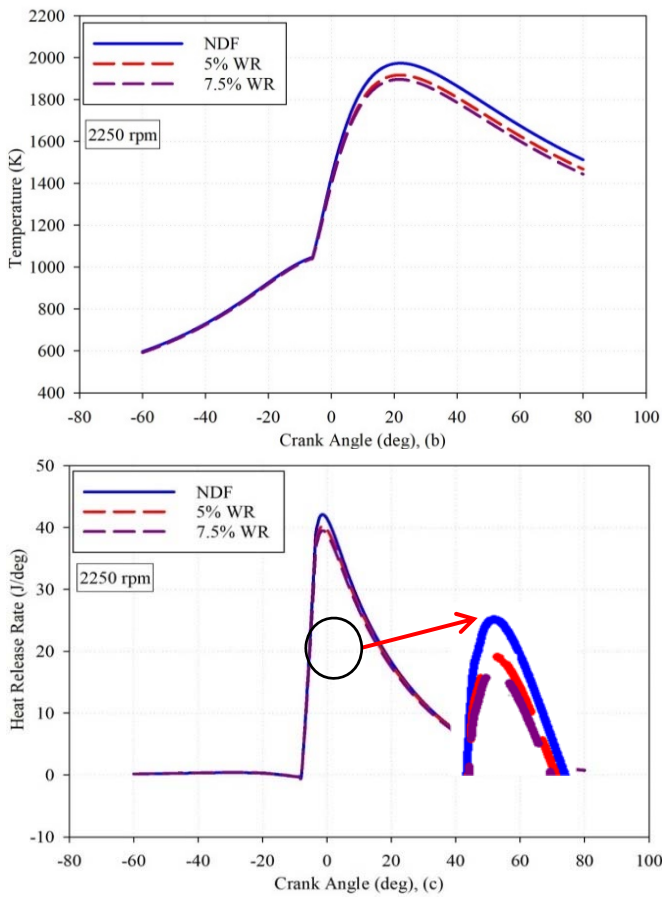


Fig. 8. Variations of **a)** cylinder pressure, **b)** cylinder temperature and **c)** HRR values obtained from the present model for NDF, 5% and 7.5% WRs at 2250 rpm

This is due to the reduction in the pressure and temperature by the effect of the vaporization of water as explained above. However, evaporation of water reduces combustion temperature and thus NO emissions. For example, as can be seen in Table 7, mole fraction values of NO for NDF, 5%, and 7.5% WRs were determined as 5.191, 4.546, and 4.340. Thus, mole fraction values of NO for 5% and 7.5% WRs were decreased by 12.43% and 16.39%, respectively, compared to NDF. As can be seen in Table 7, WAIA increases ID. WAIA application decreases the intake and the compression processes temperature values, which results in increased ID.

Renault M9R Type Diesel Engine

In another numerical application, the turbocharged Renault M9R type diesel engine with common-rail injection system, which is also used in the current 2021 model Renault Talisman automobile, has been used and the effects of WAIA in this engine have been investigated theoretically (Automobile Catalog, 2021). The main technical specifications of this engine are given in Table 8. Before investigating the effects of WAIA on this engine, the catalog values of the effective power and the fuel consumption values of this engine, and the effective power and fuel consumption values calculated from the present model were compared. The catalog value of effective power

(nominal effective power) of the Renault Talisman is given as 118 kW. The calculated effective power of this engine by using the present model is 127.27 kW. Thus, it can be seen that there is a 7.86% difference between the effective power values. The fuel consumption value of the vehicle (q_{90}) at 100 km for a constant 90 km/h velocity, is given as 4.81 L/100 km in the catalog. The calculated fuel consumption by using the present model for NDF is 4.5 L/100 km. Thus, a difference at the level of 6.88 occurred between these fuel consumption values. It can be understood from these results that the present model calculates engine performance parameters reasonably close to the catalog values of the engine for NDF. After this step, the developed model was applied to 3%, 6%, and 9% WRs under full load at 4000 rpm, which is the nominal speed. The variations of cylinder pressure, cylinder temperature, and HRR have been shown in Fig. 9 (a), (b) and (c). Also, some engine performance parameters and the mole fraction values of NO are presented in Table 9.

As can be seen in Fig. 9(a) that the tendencies of pressure curves for NDF, 3%, 6%, and 9% WRs are similar to each other and the determined maximum pressure values were 153.562, 157.721, 158.368, and 149.969 bar for NDF, 3%, 6%, and 9% WRs, respectively. For low WRs such as 3% and 6%, the cylinder pressure values increase slightly, but for 9% WR the cylinder pressure value reduces. It can be said that the use of low WAIA such as 3% and 6% improves combustion. Similar results have been reported in the relevant literature. For example, Kannan and Udayakumar (2009) stated in their numerical study that WAIA improved combustion to some extent by increasing the cylinder pressure values. The use of additives such as alternative fuels and water at low ratios is suggested by some researchers in the literature (Sahin et al., 2014; Kumar and Sharma, 2013; Vigneswaran et al., 2018). Durgun (1988); Sahin et al., (2014); and Sahin et al., (2015) have determined and suggested the most suitable ratio for ethanol and gasoline fumigation and for water was approximately 6 %, which is called the magic ratio.

As can be seen from Fig. 9(b), the temperature values for 3%, 6%, and 9% WRs are lower than that of NDF. For 3%, 6%, and 9% WRs, the maximum temperature values were reduced by 2.02%, 3.88%, and 8.14%, respectively. Numerical and experimental analysis performed in the relevant literature showed also that the presence of water vapor within the fuel-rich regions decreases the flame temperature. Thus, the chemical reaction rate in the flame zone decreases, leading to reduced temperature and pressure values. As mentioned above, any effort to decrease the cylinder temperature would contribute to a significant reduction in NO_x emissions (Sandeep et al., 2019; Gowrishankar et al., 2020; Ma et al., 2014). HRR variations as functions of CAs for 3%, 6%, and 9% WRs are shown in Fig. 9(c). As can be seen in these figures, any significant differences in the HRR profiles at the selected WRs have not been observed. However, for 3%, and 6% WRs, HRR increases, but for 9% it decreases. The maximum HRR values have increased by 5.71% and 6.15%, for 3%, and 6% WRs, respectively, and it has decreased by 6.2% at 9% WR, compared to NDF.

Table 8. Technical specifications of Renault Talisman M9R engine.

Injection system and injection Pressure	Common-rail and max: 2500 bar
Compression ratio	15.1
Cylinder bore and stroke length	85 mm and 88 mm
Number of cylinder and displacement	4 and 1997 cm ³
Maximum power and nominal engine speed	118 kW, 4000 rpm
Maximum torque and speed	360 Nm, (1500-2750) rpm

As explained before, it is thought that WAIA at low ratios such as 3% and 6% would improve the combustion process. Some substantial engine performance parameters and the mole fraction values of NO are presented in Table 9. As can be seen in this table, similar to the variation in HRR and pressure values, the effective power increases for 3% and 6% WRs, and it decreases for 9% WR. Effective power increases by 6.19% and 5.01% for 3% and 6% WRs, respectively, and decreases by 1.39% for 9% WR. For 3% and 6 % WRs, as dictated in the relevant literature, the entrainment of the air-water mixture

into the fuel spray, the evaporation, and the separation of these water molecules in the fuel spray (micro-explosion phenomena) enhance the formation of the air-fuel mixture and would enhance atomization and could promote complete combustion, which would result in an increase of in the effective power (Subramanian, 2011). According to Gowrishankar et al. (2020), there were no significant decreases in the cylinder temperature values to cause deteriorated combustion efficiency at low water ratios. However, it is thought that at a high water ratio such as 9% combustion process started to worsen.

Table 9. Effective power, BSFC, q₉₀ fuel consumption as liter at 100 km, the mole fraction values of NO, ID values for NDF and at (3-6-9)% WRs in the Renault Talisman vehicle. In addition, the ratios of increase and decrease of these values according to NDF.

4000 rpm	NDF	3% WR	Diff.(%)	6% WR	Diff.(%)	9% WR	Diff.(%)
N _c (kW)	127.27	135.15	6.19	133.65	5.01	125.50	-1.39
b _c (g/kWh)	206	208	0.97	213	3.39	223	8.25
*Y _{NO} ×1000	4.558	4.088	-10.31	3.753	-17.66	2.981	-34.20
q ₉₀ (L/100 km)	4.80	4.846	0.96	4.96	3.33	5.19	8.13
ID (°CA)	4.5237	4.7070	4.05	4.7346	4.66	4.7342	4.65

*Y_{NO} is the mole fraction of NO calculated from the chemical equilibrium. ($y_{NO} = \frac{n_{NO}}{n_T} = \frac{mol}{mol}$, n_T is the total mol number of combustion products)

Table 9 shows BSFC values and q₉₀ fuel consumption values at 100 km of Renault Talisman for NDF and selected 3%, 6%, and 9% WRs. Additionally, the variation of q₉₀ fuel consumption values at 100 km are presented in Fig. 10(a). As can be seen in this table, WAIA increases BSFC. For 3%, 6%, and 9% WRs BSFC values have increased by 0.97%, 3.39%, and 8.25%, respectively, compared to NDF. The increase ratios in BSFC for 3% and 5% WRs are lower than that of a high WR of 9%. Similarly, q₉₀ fuel consumption values at 100 km also have increased with selected WRs. q₉₀ fuel consumption as a liter at 100 km has increased from 4.8 liters to 5.13 liters for 9% WR. These results are in agreement with the results given in the relevant literature Bedford et al. (2000). As can be seen in Table 9 and Fig.10(b), WAIA decreases considerably the mole fraction of NO. The mole fraction of values NO for 3%, 6%, and 9% WRs have reduced by 10.31%, 17.66%, and 34.20%, respectively, compared to NDF.

Primarily the cylinder temperature values primarily influence the rate of formation of nitric oxide according to the well-known Zeldovich mechanism (Heywood, 1988). Thus, any effort to decrease cylinder temperature would result in beneficial effects to reduce the mole fraction of NO. As it is known from the relevant literature, the use of water in diesel engines is one of the most effective methods to reduce NO emission without worsening BSFC (Kökkülünk, 2012; Ma et al., 2014). For example, Kannan and Udayakumar (2009) stated that they achieved approximately 20% reductions in NO emission by adding water as diesel-water emulsion in their numerical study.

The ID values for NDF and selected WRs are given in Table 8. ID values for 3%, 6%, and 9% WRs increase by 4.05%, 4.66%, and 4.65%, respectively, compared to NDF. With the WAIA application, the temperature values during fuel injection would be lower because injected water during the intake stroke will vaporize and cool the air, which leads to a rise in ID. Also, increasing ID may cause more fuel to be burned around TDC. It is well-known in the literature that without knocking the burning of fuel around TDC increases the effective power and efficiency of diesel engines (Heywood, 1988; Durgun, 2022).

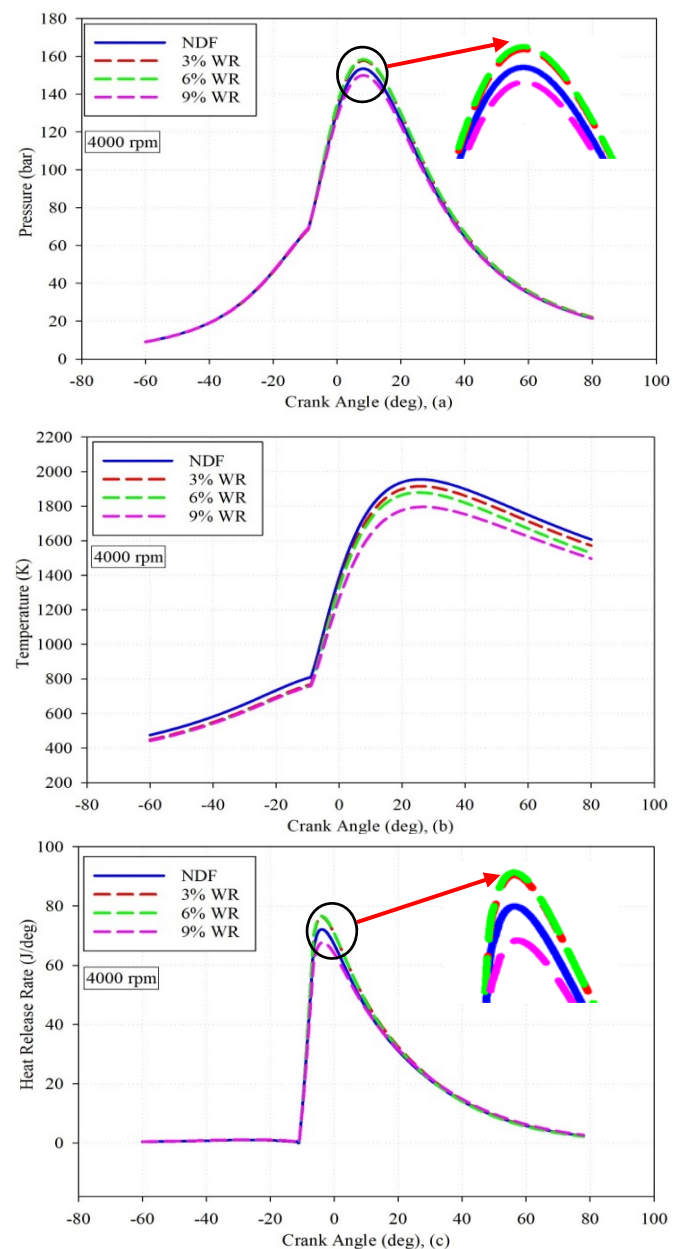


Fig. 9. Variations of a) cylinder pressure, b) cylinder temperature and c) HRR obtained from the presented model for NDF, 3%, 6% and 9% WRs at 4000 rpm in the M9R type diesel engine used in Renault Talisman automobile

CONCLUSIONS

In this study, a computer code based on the thermodynamic-based ZDSZ model originally proposed and given by Ferguson (1986) for diesel engine cycles has been improved with some additional modifications for NDF and WAIA. This developed model can calculate diesel engine cycles with sufficient accuracy for NDF and WAIA. The accuracy control results of this model and the results of the applications for water adding into intake air at different ratios, on engine performance and NO emission in two different automotive diesel engines are briefly given below.

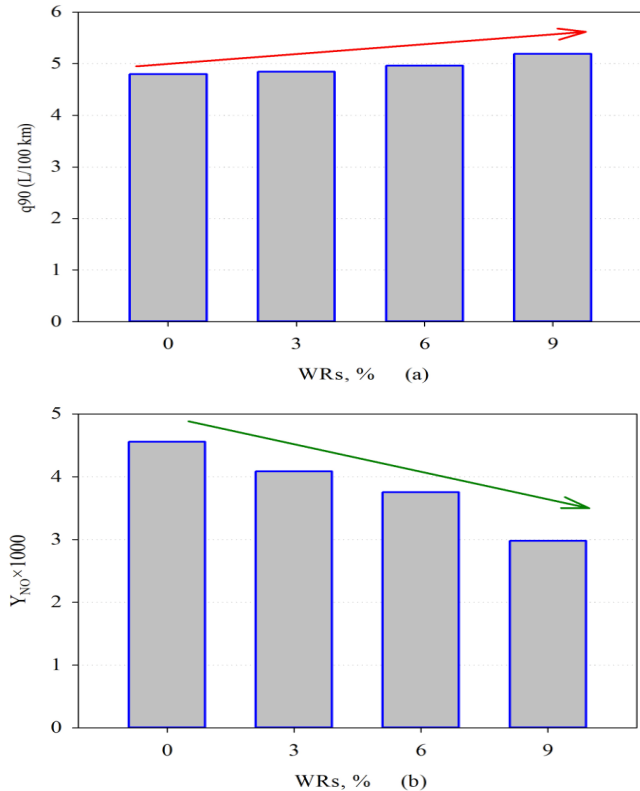


Fig. 10. Variations of (a) q_{90} fuel consumption as liter at 100 km and (b) the mole fraction values of NO versus different WRs at 4000 rpm in the M9R type diesel engine used in Renault Talisman automobile

1. The accuracy of our model was validated using experimental data from tests conducted at 2000 rpm and 4000 rpm, with 6% and 10% WAIA levels. For instance, at 2000 rpm, the maximum pressure difference between our model and experimental results was 1.1% for 6% WAIA, and 1.2% for 10% WAIA. Similar differences were observed at 4000 rpm. Overall, differences in cylinder pressure, temperature, and heat release rate ranged from 0.02% to 12.14% across all conditions.

2. The present model could calculate motor performance parameters with sufficient accuracy for NDF and WAIA. The q_{90} fuel consumption value of the Renault Talisman at 100 km for 90 km/h constant velocity is given as 4.81 L in the vehicle catalog. The calculated fuel consumption by using the present model for NDF is obtained as 4.5 L. Thus, a 6.88 % difference was calculated between the q_{90} fuel consumption values.

3. The results obtained at the end of the numerical study for two different automotive diesel engines can be summarized separately as follows. In the first application, the developed model has been applied for NDF, 5%, and 7.5% WRs at 2250 rpm in Renault K9K-700 type diesel engine.

3.a) WAIA decreases cylinder pressure, temperature, and HRR values for selected operating conditions for this engine. For 5% and 7.5% WRs, cylinder temperature values, and the maximum HRR ratios have decreased by (2.87%, and 3.91%) (4.46% and 6.22%), respectively, compared to that of NDF.

3.b) WAIA reduces effective power and NO emissions but increases BSFC for this engine. Compared to NDF, effective power and NO emissions decreased by (4.26%, 7.37%) and (12.43%, 16.39%) for 5% and 7.5% WRs, respectively. Meanwhile, BSFC increased by 6.95% and 10.56% for 5% and 7.5% WRs, respectively. Additionally, ID values slightly increased with WAIA at 2250 rpm.

4. The second numerical application was made for the Talisman automobile engine and the numerical comparison results obtained from the present model at 3%, 6%, and 9% at 4000 rpms in this engine are given below.

4.a) 3% and 6% WRs increase slightly the cylinder pressure values, but 9% WR reduces the cylinder pressure values. For 3% and 6% WRs, the increase ratio of maximum pressure values compared to NDF was determined as 2.71% and 3.13%, respectively. At 9% WR, the decrease ratio of maximum pressure value was calculated as 2.34%.

4.b) 3%, 6%, and 9% WRs reduce the cylinder temperature values. For 3%, 6%, and 9% WRs, the maximum temperature values decreased by 2.02%, 3.88%, and 8.14%, respectively.

4.c) For 3 % and 9 % WRs, HRR increase, but for 9 % it decreases. The maximum HRR values have increased by 5.71% and 6.15%, for 3 % and 6% WRs, respectively, but it has decreased by 6.2% at 9% WR, compared to NDF.

4.d) BSFC values and the q_{90} fuel consumption values at 100 km of Renault Talisman increase with application of 3%, 6%, and 9% WAIA. For 3%, 6%, and 9% WRs BSFC values have increased by 0.97%, 3.39%, and 8.25%, respectively, compared to NDF.

4.e) WAIA decreases considerably NO emissions of this engine. NO emission values for 3%, 6%, and 9% WRs have reduced by 10.31%, 17.66%, and 34.20%, respectively, compared to NDF.

4.f) WAIA increases ID values in this engine. ID values for 3%, 6%, and 9% WRs increase by 4.05%, 4.66%, and 4.65%, respectively, compared to NDF.

REFERENCES

- Automobile Catalog, 2021. (Accessed 8. November. 2021). https://www.automobilecatalog.com/car/2022/2986985/renault_talisman_blue_dci_160_edc.html#gsc.tab=0.
- Bedford, F.W.F., C. Rutland, P. Dittrich, A. Raab. 2000. Effects of direct water injection on DI diesel engine combustion. *SAE Tech. Pap. 01:12*. <https://doi.org/https://doi.org/10.4271/2000-01-2938>.
- Bondar, V., S. Aliukov, A. Malozemov, A. Das. 2020. Mathematical model of thermodynamic processes in the intake manifold of a diesel engine with fuel and water injection. *Energies* 13(17):4315. <https://doi.org/10.3390/en13174315>.

- Borman, G.L., and K.W. Ragland. 1998. Combustion Engineering, McGraw-Hill. <https://books.google.com.tr/books?id=ZxdFPgAACAAJ>.
- Butcher, J.C., 1995. On fifth order Runge-Kutta methods, *BIT Numerical Mathematics* 35:202–209. <https://doi.org/10.1007/BF01737162>.
- Durgun, O. 1988. Using Ethanol in Spark Ignition Engine, *UCTEA Chamb. Mech. Eng. J.* 29: 24–26.
- Durgun, O. 1990. Experimental Methods in the Internal Combustion Engines.
- Durgun, O. 1991. A practical method for calculation engine cycles, *Union Chambers Turkish Eng. Arc., Chamb. Mech. Eng.* 383:18–29.
- Durgun, O. 2022. Internal Combustion Engines Basic Principles, Turkish Chamber of Naval Architect and Marine Engineers.
- Ece, Y.M., and V. Ayhan. 2019. Investigation of the Effect of Direct Water Injection on Performance and Emissions of a Single Cylinder Diesel Engine. *J. Adv. Technol. Sci.* 8: 11–21. (In Turkish). <https://dergipark.org.tr/tr/download/article-file/719644>
- Ferguson, C. R., 1986. Internal Combustion Engines Applied Thermodynamics.
- Gowrishankar, A.K.S., P. Bhasker J, and P. Rastogi. 2020. Investigations on NO_x and smoke emissions reduction potential through water-in-diesel emulsion and water fumigation in a small-bore diesel engine, *SAE Tech. Pap.* 32:12. <https://doi.org/https://doi.org/10.4271/2020-32-2312>.
- Heywood, J. B., 1988. Internal Combustion Engine Fundamentals.
- Jhalani, A., D. Sharma, S.L. Soni, P.K. Sharmai. 2023. Effects of process parameters on performance and emissions of a water-emulsified diesel-fueled compression ignition engine. *Energy Sources, Part A Recover. Util. Environ. Eff.* 45:4242–4254. <https://doi.org/10.1080/15567036.2019.1669739>.
- Jurić, F., M. Krajcar, N. Duić, M. Vujanović. 2023. Investigating the pollutant formation and combustion characteristics of biofuels in compression ignition engines: A numerical study. *Therm. Sci. Eng. Prog.* 43:101939. <https://doi.org/10.1016/J.TSEP.2023.101939>.
- Kannan, K., M. Udayakumar. 2009. Modeling of nitric oxide formation in single cylinder direct injection diesel engine using diesel-water emulsion. *Am. J. Appl. Sci.* 6:1313–1320. <https://doi.org/10.3844/ajassp.2009.1313.1320>.
- Khatrı, D., and R. Goyal. 2020. Performance, emission and combustion characteristics of water diesel emulsified fuel for diesel engine: A review. *Mater. Today Proc.* 28: 2275–2278. <https://doi.org/10.1016/J.MATPR.2020.04.560>.
- Kökkülünk, G. 2012. Analysis of the Effects of Exhaust Gas Recirculation (EGR) on Diesel Engine with Steam Injection System to Performance and Emission Parameters, YTU, (In Turkish Thesis).
- Kökkülünk, G., G. Gonca, V. Ayhan, I. Cesur, A. Parlak. 2013. Theoretical and experimental investigation of diesel engine with steam injection system on performance and emission parameters. *Appl. Therm. Eng.* 54:161–170. <https://doi.org/10.1016/J.APPLTHERMALENG.2013.01.034>
- Kumar, V.V.N, and A. Sharma. 2013. Performance analyses of diesel engine at different injection angles using water diesel emulsion, *SAE Tech. Pap.* 01:10. <https://doi.org/https://doi.org/10.4271/2013-01-2170>
- Lamas, M.I., C.G. Rodríguez, J.D. Rodríguez, J. Telmo. 2013. Internal modifications to reduce pollutant emissions from marine engines. A numerical approach, *Int. J. Nav. Archit. Ocean Eng.* 5:493–501. <https://doi.org/10.2478/IJNAOE-2013-0148>.
- Ma, X., F. Zhang, K. Han, Z. Zhu, Y. Liu. 2014. Effects of intake manifold water injection on combustion and emissions of diesel engine. *Energy Procedia* 61:777–781. <https://doi.org/10.1016/J.EGYPRO.2014.11.963>.
- Maawa, W.N., R. Mamat, G. Najafi, L.P.H. De Goey. 2020. Performance, combustion, and emission characteristics of a CI engine fueled with emulsified diesel-biodiesel blends at different water contents. *Fuel* 267:117265. <https://doi.org/10.1016/J.FUEL.2020.117265>.
- Nemati, P., S. Jafarmadar, and H. Taghavifar. 2016. Exergy analysis of biodiesel combustion in a direct injection compression ignition (CI) engine using quasi-dimensional multi-zone model, *Energy* 115:528–538. <https://doi.org/10.1016/J.ENERGY.2016.09.042>.
- Parlak, A., G. Gonca, Y. Üst, B. Sahin, A. Safa. 2019. A comprehensive comparison of steam injected diesel engine and miller cycled diesel engine by using two zone combustion model. *Journal of the Energy Institute* 88(1):43-52. <https://doi.org/10.1016/j.joei.2014.04.007>.
- Pasternak, M., F. Mauss, and H. Bensler. 2009. Diesel engine cycle simulation with a reduced set of modeling parameters based on detailed kinetics. *SAE Tech. Pap.* 01:13. <https://doi.org/https://doi.org/10.4271/2009-01-0676>.
- Qiong, Li. 1992. Development of a quasi-dimensional diesel engine simulation for energy and availability analysis. University of Illinois at Urbana-Champaign. Doktoral thesis.
- Rajak, U., P. Nashine, T.S. Singh, T.N. Verma. 2018. Numerical investigation of performance, combustion and emission characteristics of various biofuels. *Energy Convers. Manag.* 156: 235–252. <https://doi.org/10.1016/J.enconman.2017.11.017>.
- Rakopoulos, C.D., K.A. Antonopoulos, D.C. Rakopoulos, D.T. Hountalas. 2008. Multi-zone modeling of combustion and emissions formation in DI diesel engine operating on ethanol–diesel fuel blends. *Energy Conversion and Management.* 49:625–643. <https://doi.org/10.1016/J.enconman.2007.07.035>.
- Sahin, Z., M. Tuti, and O. Durgun. 2014. Experimental investigation of the effects of water adding to the intake air on the engine performance and exhaust emissions in a DI automotive diesel engine. *Fuel* 115:884–895. <https://doi.org/10.1016/J.FUEL.2012.10.080>.
- Sahin, Z., and O. Durgun. 2008. Multi-zone combustion modeling for the prediction of diesel engine cycles and engine performance parameters. *Appl. Therm. Eng.* 28:2245–2256. <https://doi.org/10.1016/J.APPLTHERMALENG.2008.01.002>

- Sahin, Z., O. Durgun, and M. Tuti. 2018. An experimental study on the effects of inlet water injection of diesel engine heat release rate, fuel consumption, opacity, and NO_x emissions, *Exergetic, Energ. Environ. Dimens.* 981–996.
<https://doi.org/10.1016/B978-0-12-813734-5.00055-X>.
- Sahin, Z., O. Durgun, and O.N. Aksu. 2015. Experimental investigation of n-butanol/diesel fuel blends and n-butanol fumigation-evaluation of engine performance, exhaust emissions, heat release and flammability analysis. *Energy Convers. Manag.* 103 778–789.
<https://doi.org/10.1016/J.enconman.2015.06.089>.
- Sandeep, S., D.S. Kumar, S. Krishnan, S.K. Pandey. 2019. Assessment of atomized water injection in the intake manifold of a heavy duty diesel engine for NO_x reduction potential. *IOP Conf. Ser. Mater. Sci. Eng.* 577:12186.
<https://doi.org/10.1088/1757-899X/577/1/012186>.
- Savioli, T. 2015. CFD analysis of 2-stroke engines. *Energy Procedia.* 81:723–731.
<https://doi.org/10.1016/J.EGYPRO.2015.12.078>.
- Senčić, T., V. Mrzljak, P. Blecich, I. Bonefačić. 2019. 2D CFD simulation of water injection strategies in a large marine engine. *J. Mar. Sci. Eng.* 7:296.
<https://doi.org/10.3390/jmse7090296>.
- Shrivastava, R., R. Hessel, and R.D. Reitz. 2002. CFD optimization of DI diesel engine performance and emissions using variable intake valve actuation with boost pressure, EGR and multiple injections. *SAE Tech. Pap.* 111:1612-1629.
<https://doi.org/10.4271/2002-01-0959>.
- Sindhu, R., G.A.P. Rao, and K.M. Murthy. 2014. Thermodynamic modelling of diesel engine processes for predicting engine performance. *Int. J. Appl. Eng. Technology.* 4:101-114.
<https://api.semanticscholar.org/CorpusID:56402776>.
- Subramanian, K.A. 2011. A comparison of water–diesel emulsion and timed injection of water into the intake manifold of a diesel engine for simultaneous control of NO and smoke emissions. *Energy Conversion Management.* 52:849–857.
<https://doi.org/10.1016/J.enconman.2010.08.010>.
- Tamma, B., J.C. Alvarez, and A.J. Simon. 2003. Water Addition in Diesel Engine Intake for NO_x Reduction: Comparison of Modeling and Experiments. *Internal Combustion Engine Division Fall Technical Conference (ICEF)*, 0749:245–249.
<https://doi.org/10.1115/ICEF2003-0749>.
- Tauzia, X., A. Maiboom, and S.R. Shah. 2010. Experimental study of inlet manifold water injection on combustion and emissions of an automotive direct injection Diesel engine. *Energy* 35:3628–3639.
<https://doi.org/10.1016/J.energy.2010.05.007>.
- Tutak, W., and A. Jamrozik. 2016. Validation and optimization of the thermal cycle for a diesel engine by computational fluid dynamics modeling. *Appl. Math. Model* 40:6293–6309.
<https://doi.org/10.1016/J.APM.2016.02.021>.
- Tuti, M. 2012. Experimental Investigation of the Effects of Water Adding to the Intake Air on the Engine Performance and Exhaust Emissions in a Diesel Engine, Karadeniz Technical University, Master thesis. (In Turkish).
- Tuti, M. 2022. Experimental and Numerical Investigation of the Effects of Adding Water to the Intake Air on Engine Performance, Combustion and Exhaust Emissions in Diesel Engines. Karadeniz Technical University. Doktoral thesis (In Turkish).
- Vellaiyan, S., A. Subbiah, and P. Chockalingam. 2019. Multi-response optimization to obtain better performance and emission level in a diesel engine fueled with water-biodiesel emulsion fuel and nanoadditive. *Environment Science Pollution Reserch* 26:4833–4841.
<https://doi.org/10.1007/s11356-018-3979-6>.
- Vigneswaran, R., K. Annamalai, B. Dhinesh, R. Krishnamoorthy. 2018. Experimental investigation of unmodified diesel engine performance, combustion and emission with multipurpose additive along with water-in-diesel emulsion fuel. *Energy Convers. Manag.* 172: 370–380.
<https://doi.org/10.1016/J.enconman.2018.07.039>.
- Wang, Z., S. Wu, Y. Huang, S. Huang, S. Shi, X. Cheng, R. Huang. 2018. Experimental investigation on spray, evaporation and combustion characteristics of ethanol-diesel, water-emulsified diesel and neat diesel fuels, *Fuel* 231:438–448.
<https://doi.org/10.1016/J.FUEL.2018.05.129>.
- Woschni, G. 1967. A Universally applicable equation for the instantaneous heat transfer coefficient in the internal combustion engine. *SAE Tech. Pap.* 670931:19.
<https://doi.org/https://doi.org/10.4271/670931>.
- Zhang, J., Y.Meng, D.Liu, L.Liu, X.Ma, C. Jiang, X. Li, L. Huang. 2023. Modelling and multi-objective combustion optimization of marine engine with speed maintaining control target. *Therm. Sci. Eng. Prog.* 41:101852.
<https://doi.org/10.1016/J.TSEP.2023.101852>.
- Zhu, S., B. Hu, S. Akehurst, C. Copeland, A. Lewis, H. Yuan, I. Kennedy, J. Bernards, C. Branney. 2019. A review of water injection applied on the internal combustion engine, *Energy Convers. Manag.* 184:139–158.
<https://doi.org/10.1016/J.enconman.2019.01.042>.